

## **Graphene oxide-controlled neutral *versus* cationic form of a red emitting dye: enhancement of fluorescence by graphene oxide**

### **Contents.**

**S1.** Experimental Section.

**Scheme.S1** GO responsive colour changes of NBA in DMSO.

**Scheme.S2** GO responsive colour changes of NBA in THF.

**S2.** Ground-state absorption spectral studies.

**S3.** Fluorescence emission spectral studies.

**S4.** Time-resolved fluorescence emission spectral studies.

**S5.** Raman spectral study of GO-NBA conjugate in different solvent media.

**S6.** FLIM study of NBA-GO complex systems in different solvent media.

**S7.** Computational studies to probe the interaction of NBA, NBB with GO.

## **S1. Experimental Section**

### **S1.1. Materials.**

NBA and graphene oxide (GO) were procured from Sigma Aldrich and used without further purification. Dimethyl sulfoxide (DMSO), tetrahydrofuran (THF), and methanol used in our study, all are spectral grade solvents and purchased from SRL India. Here we have used triple distilled water.

### **S1.2 Sample Preparation.**

For all spectroscopic measurements, we have fixed the concentration of NBA as 3 $\mu$ M. 2mg of GO was dissolved in 4 ml of neat solvent, to prepare 2mg/4ml GO stock solution. After the addition of GO in the respective neat solvent, we have sonicated it for atleast 2 hours. During the sonication we have fixed the temperature of the sonicator at 10<sup>o</sup> C, to minimize the extra heat that was generated during the sonication. As prepared 2mg/4ml GO stock solution of the required amount was added dropwise into the cuvette. During all measurements, we have used a freshly prepared sample solution.

### **S1.3 Instrumentation.**

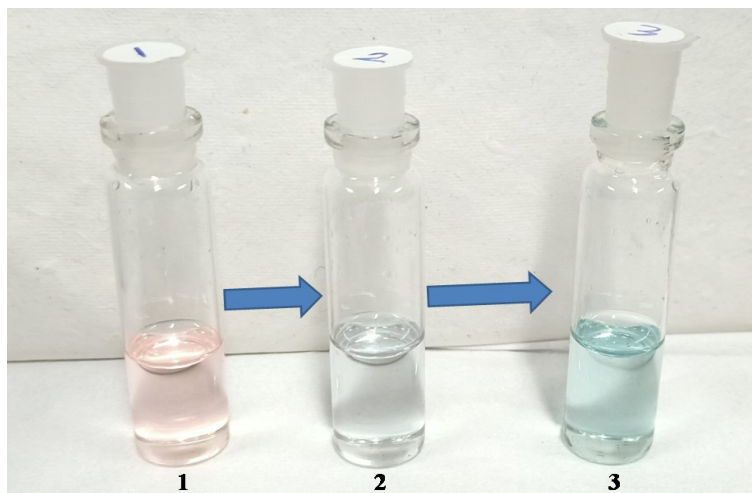
We have acquired the absorption spectra of our experiments in a UV-Vis spectrophotometer made by Shimadzu and emission spectra of our experiments were acquired using a spectrofluorometer made by Horiba JobinYvon. All of our experiments were measured at a fixed temperature of 298 K. A picosecond time-correlated single-photon counting (TCSPC) spectrometer was used to collect the time-resolved emission decays, using diode laser of 635, 510 nm excitation wavelengths. Fluorescence lifetime imaging (FLIM) experiments were carried out using a commercially available DCS-120 confocal microscope system made by Becker and Hickl (GmbH). For the FLIM measurements, samples were excited by using 635, 510 nm diode lasers. For the focussing of the samples, before FLIM measurements we have used an optical microscope that is inverted in nature, and a galvo-drive unit made by Becker and Hickl was controlling it. For the focusing of our samples, we have used a 40X objective with nile aperture of 0.75. Here we have used a hybrid GaAsP photodetector as a detector. The instrument response function (IRF) of the instrument is <100 ps.

### **S1.4 Detailed procedure for computational studies.**

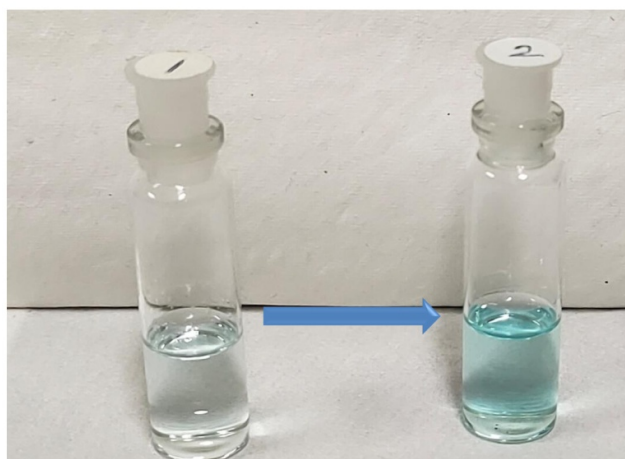
In this present work, in order to find out the preferable site for interactions in between the NBA molecule on the GO surface we perform computational studies by using the Gaussian 16 suite of programme.<sup>51</sup> Our model structure of GO contains one epoxy, three hydroxyl groups in its basal plane, and one carboxylic acid group in its edge. The exactly same model structure of GO were used by several research groups recently.<sup>52,53</sup> We first optimized the NBA and GO molecules separately, and then we doped the NBA molecule in the surface of GO skeleton in two orientations. In forward orientation the naphthylamine moiety of dye molecule (containing NH<sub>2</sub> group) is placed over the -COOH group of GO surface and in

reverse orientation where the  $\text{NEt}_2$  group is situated over the  $\text{-COOH}$  group of GO surface. Optimizations of all the molecules are carried out in gas as well as solvent phases. Both types of interactions i.e; forward orientation and reverse orientation in between NBA molecule and GO skeleton are also carried out in gas as well as in solvent phases. In our study we considered four different solvents including two protic and two aprotic solvents. Computational studies are carried out with the help of density functional theory and all the geometries are optimized at M052X/6-31+G(d,p) level of theory using Gaussian 16 programme. Binding energy is calculated by using the formula given below-

$$BE = E_{GO:NBA} - [E_{GO} + E_{NBA}] \dots \dots \dots (1)$$



**Scheme.S1** GO induced colour changes of NBA in DMSO (1) 3 $\mu\text{M}$  NBA in DMSO (light pink), (2) 3 $\mu\text{M}$  NBA in DMSO+ 7  $\mu\text{g/ml}$  GO (colourless), (3) 3 $\mu\text{M}$  NBA in DMSO+ 15  $\mu\text{g/ml}$  GO (light blue colour).



**Scheme.S2** GO induced colour changes of NBA in THF (1) 3 $\mu\text{M}$  NBA in THF (colourless), (2) 3 $\mu\text{M}$  NBA in THF+ 10  $\mu\text{g/ml}$  GO (cyan colour).

S2. Absorption spectral studies.

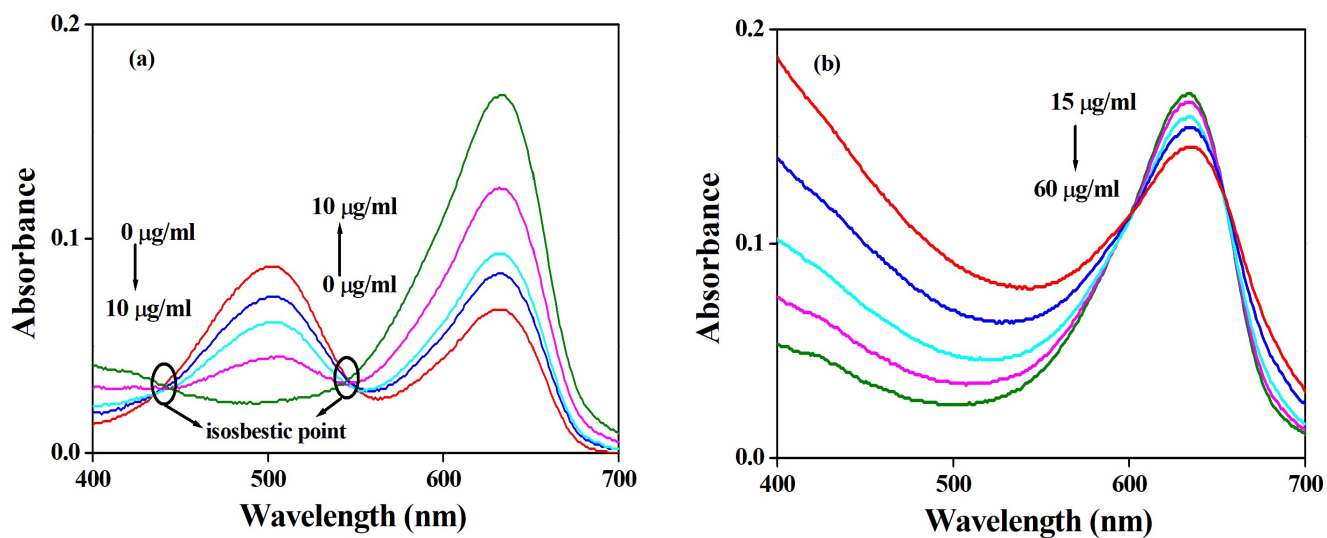


Fig.S1 (a) Absorption spectral profile of NBA upto the addition of (0-10  $\mu\text{g/ml}$ ) GO in THF, (b) Absorption spectral profile of NBA upto the addition of (15-60  $\mu\text{g/ml}$ ) GO in THF.

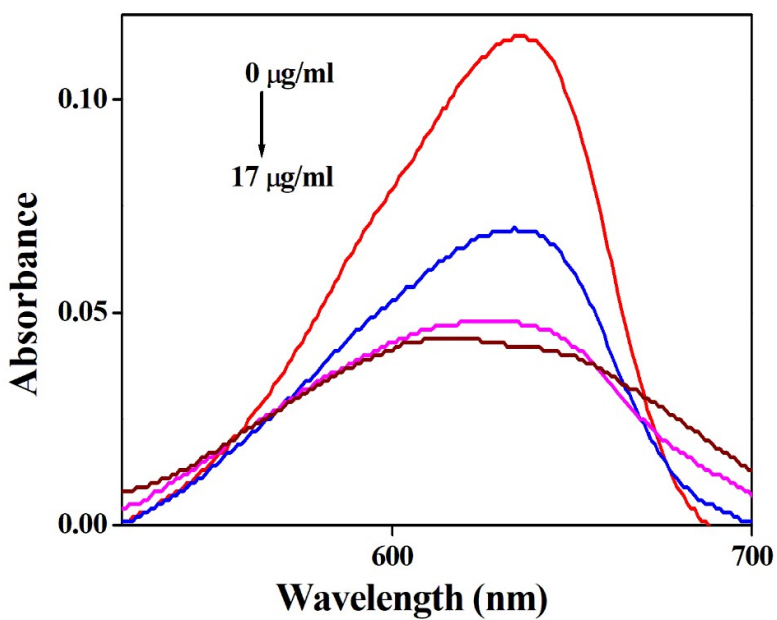


Fig.S2 Absorption spectral profiles of NBA with the addition of (0-17 $\mu\text{g/ml}$ ) GO in water.

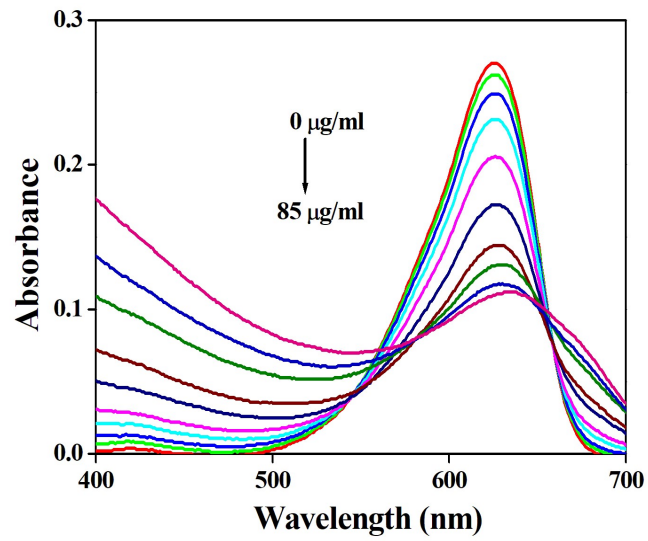
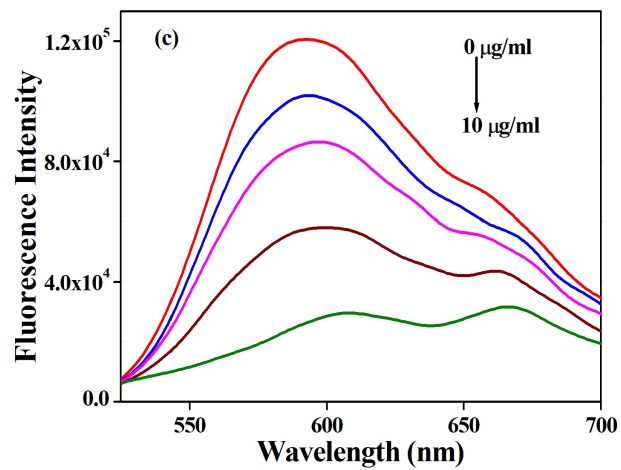
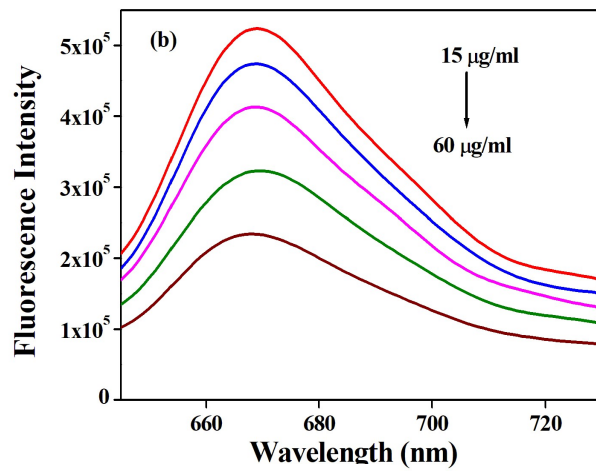
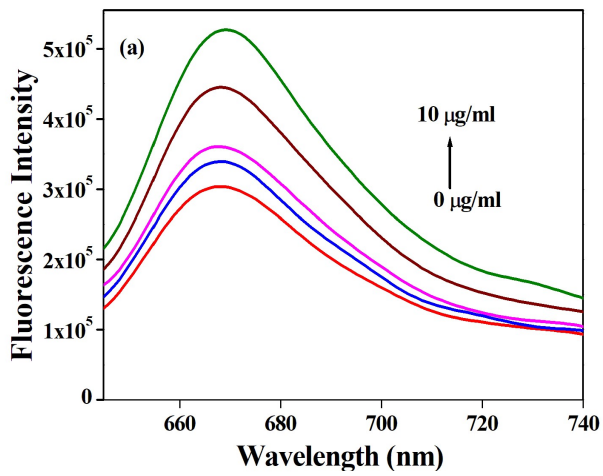


Fig.S3 Absorption spectral profiles of NBA with the addition of (0-85 $\mu\text{g/ml}$ ) GO in methanol.

S3. Fluorescence emission spectral studies.



**Fig.S4** (a) Fluorescence emission spectral profile of NBA upto the addition of (0-10  $\mu\text{g/ml}$ ) GO in THF, at  $\lambda_{\text{ex}}=635$  nm. (b) Fluorescence emission spectral profile of NBA upto the addition of (15-60  $\mu\text{g/ml}$ ) GO in THF, at  $\lambda_{\text{ex}}=635$  nm. (c) The fluorescence emission spectral profile of NBA upto the addition of (0-10  $\mu\text{g/ml}$ ) GO in THF, at  $\lambda_{\text{ex}}=500$  nm.

It is also noticeable that the quenching efficiency of GO is much higher in water, as in water after the addition of 17  $\mu\text{g/ml}$  GO, the emission intensity of NBA was quenched  $\sim 11$  times of its original, whereas in methanol after the addition of 85  $\mu\text{g/ml}$  GO, the emission intensity of NBA was quenched  $\sim 11$  times of its original.

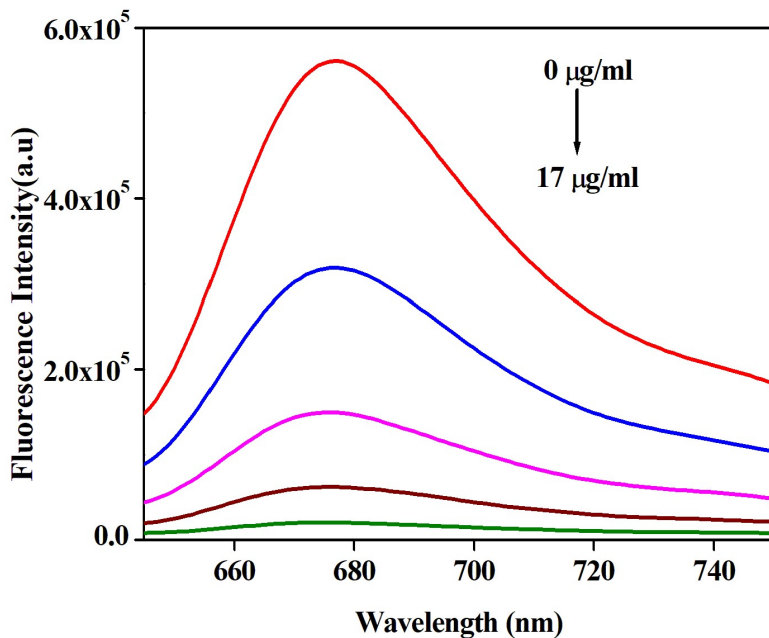


**Fig.S5** Fluorescence emission spectral profiles of NBA with the addition of (0-17  $\mu\text{g/ml}$ ) GO in  $\text{H}_2\text{O}$ , at  $\lambda_{\text{ex}}=635$  nm.

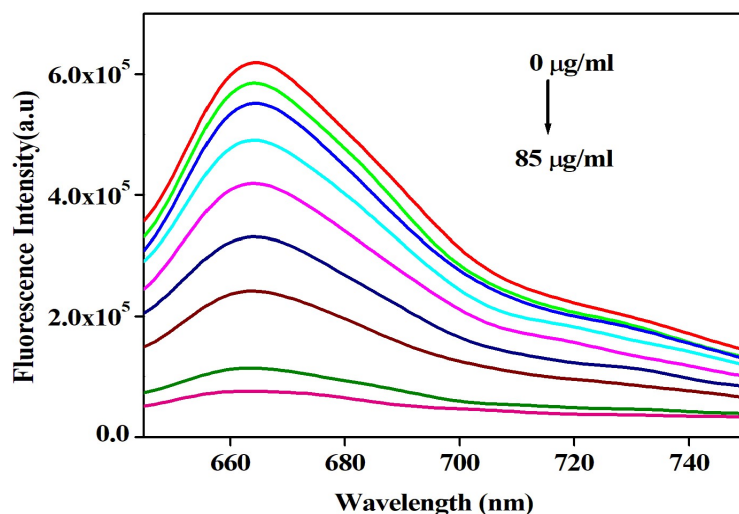


**Fig.S6** Fluorescence emission spectral profile of NBA upto the addition of (0-85  $\mu\text{g/ml}$ ) GO in methanol, at  $\lambda_{\text{ex}}=635$  nm.

#### S4. Time-resolved fluorescence emission spectral studies.

Time-resolved fluorescence emission spectral study of NBA after the addition of GO in DMSO (at  $\lambda_{\text{ex}}=635, 510$  nm) were carried out by us. The decay profiles of NBA in neat DMSO and after the addition of GO were best fitted bi-exponentially, at  $\lambda_{\text{ex}}=635$ . The obtained lifetime components and their corresponding relative weight percentages were remains the same after the addition of GO at  $\lambda_{\text{ex}}=635$  (**Table.S1**). Upto the addition of 15  $\mu\text{g/ml}$  GO the proportion of NBA increases only, and as a result, the average lifetime of NBA in DMSO after the addition of 15  $\mu\text{g/ml}$  GO remains the same, at  $\lambda_{\text{ex}}=635$ . However, after the additions of 20  $\mu\text{g/ml}$  GO, GO quenches the NBA fluorescence via static quenching and as a result upto the addition of 90  $\mu\text{g/ml}$  GO, the average lifetime remains the same as that of NBA in neat DMSO (**Fig.S7a**). But the scenario was totally different when we excited NBA at  $\lambda_{\text{ex}}=510$  nm in DMSO medium in the presence of GO. The average lifetime of NBA in the presence of GO enhanced upto the addition of 15  $\mu\text{g/ml}$  GO compared to NBA in neat solvent (**Table.S2, Fig.S7b**). One interesting observation is that the average lifetime of NBA at  $\lambda_{\text{ex}}=510$  nm, after the addition of 15  $\mu\text{g/ml}$  GO was close to that of NBA in neat DMSO at  $\lambda_{\text{ex}}=635$  nm. This also clarified that after the addition of 15  $\mu\text{g/ml}$  GO, in the excited-state due to proton transfer from GO surface to NBB, NBB molecules were converted to NBA and as a result, the average lifetime values of NBA at both excitation wavelengths became the same. The decay profiles of NBA in neat DMSO and in the presence of GO at  $\lambda_{\text{ex}}=510$  nm were best-fitted tri-exponentially. Tri-exponential fitting indicates the presence of three species in the medium at  $\lambda_{\text{ex}}=510$  nm. We predict that the species will be NBB, NBA, and (NBB.....H.....DMSO)<sup>+</sup> for neat solvent and (NBB.....H.....GO)<sup>+</sup> when it forms complex with GO. We also predict that the fastest component is due to (NBB.....H.....GO)<sup>+</sup>, intermediate and slowest components are due to the NBB and NBA respectively. It was observable that the first lifetime component remains more or less the same after the addition of GO (**Table.S2**) and its relative weight percentage enhanced progressively (from 45% in neat DMSO to 68% after the addition of 15  $\mu\text{g/ml}$  GO) with the gradual addition of GO. However, the intermediate component enhanced (from 1.44 ns in neat DMSO to 1.86 ns after the addition of 15  $\mu\text{g/ml}$  GO) and relative weight percentage decreases (from 12% in neat DMSO to 8% after the addition of 15  $\mu\text{g/ml}$  GO) in a little extent with the gradual addition of GO. This Indicates that the proportion of NBB decreases. However, our assumptions fail for the case of the slowest component (although it may be clearer for the case of THF). As we discuss the slowest component is may be due to the NBA form. So it is clear that the relative weight percentage of the slowest component must have enhanced after the gradual addition of GO. But we found that in DMSO, although the slowest component enhanced (from 2.30 ns in neat DMSO to 4.10 ns after the addition of 15  $\mu\text{g/ml}$  GO) but its relative weight percentage decreases (from 43% in neat DMSO to 24% after the addition of 15  $\mu\text{g/ml}$  GO).

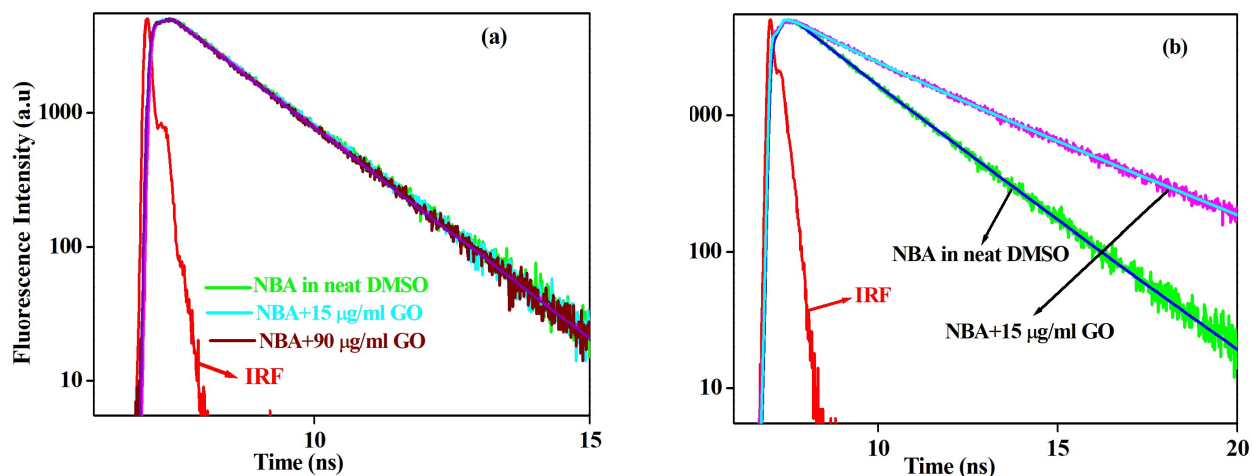


**Fig.S7** Time-resolved fluorescence emission decay traces of NBA in DMSO, with gradual addition of GO (a) at  $\lambda_{ex}=635$  nm and (b) at  $\lambda_{ex}=510$  nm.

Similar kinds of observation were executed by us for the case of THF at  $\lambda_{ex}=635$  nm. The decay profiles of NBA in neat THF and after addition of GO were best fitted bi-exponentially, at  $\lambda_{ex}=635$ . The obtained lifetime components and their corresponding relative weight percentages were remains the same after the addition of GO at  $\lambda_{ex}=635$  (Table.S1, Fig.S8a). As a result, the average lifetime of NBA in neat THF and after addition of GO remains the same at  $\lambda_{ex}=635$  nm. But the observation at  $\lambda_{ex}=510$  nm for THF is quite different from that of DMSO (Fig.S8b). Like DMSO, in THF the decay profile of NBA fitted tri-exponentially. However, the gradual addition of GO in NBA shows that the lifetime components of NBA remain more or less the same only the relative weight percentages of the components modified (Table.S2). As we predict that the fastest component is due to  $(NBB \dots H \dots GO)^{\dagger}$ , intermediate and slowest components are due to NBB and NBA respectively, it will be clear from here. The fastest lifetime component of NBA in neat THF observed as 0.05 ns (62%). After the addition of 10  $\mu\text{g/ml}$  of GO, the fastest component remains the same and its relative weightage decreased in a little extent (Table.S2). Similarly, the intermediate lifetime component in the absence and presence of GO remains more or less same only the relative weight percentage of the component decreases from 32% in neat THF to 5% in the presence of 10  $\mu\text{g/ml}$  of GO. As we discussed the intermediate component is due to NBB form, so after the gradual addition of GO due to excited-state proton transfer from GO to NBB, the NBB molecules were converted to NBA and as a result, relative weight percentages of the intermediate component decreases. However, due to protonation of NBB in the presence of GO, the relative weight percentages of the slowest component enhanced (from 6% in neat DMSO to 36% after the addition of 10  $\mu\text{g/ml}$  GO) without changing the magnitude of the slowest component, indicates that proportion of NBA enhanced in the solution. Like DMSO, in THF we found that the average lifetime of NBA at  $\lambda_{ex}=510$  nm, after the addition of 10  $\mu\text{g/ml}$  GO was similar to that of NBA in neat THF at  $\lambda_{ex}=635$  nm.



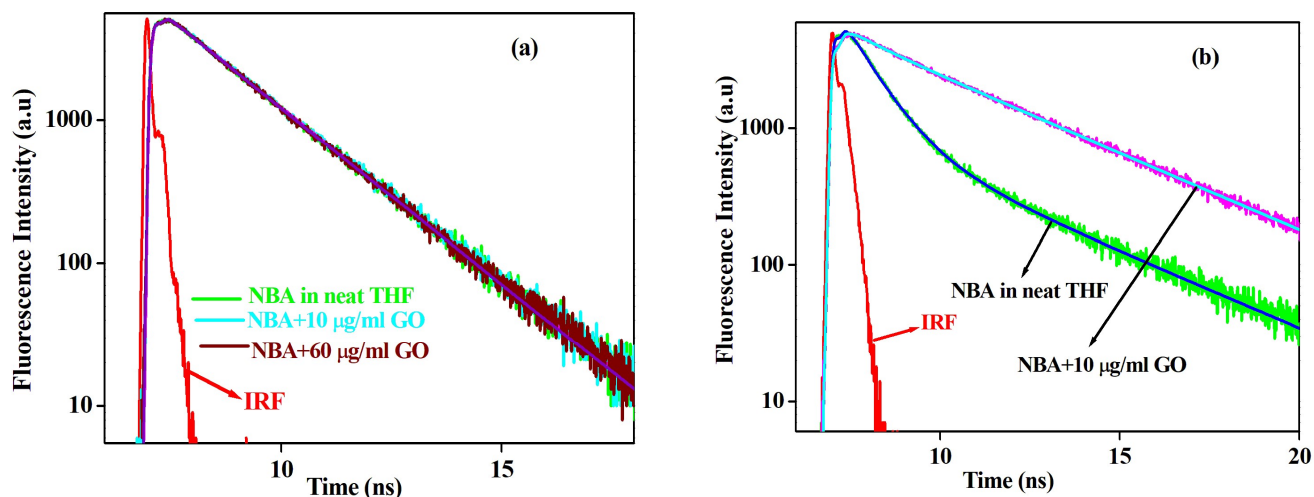


**Fig.S8** Time-resolved fluorescence emission decay traces of NBA in THF, with gradual addition of GO (a) at  $\lambda_{ex}=635$  nm and (b) at  $\lambda_{ex}=510$  nm.

The time-resolved fluorescence emission spectral study of NBA with the gradual addition of GO in water and methanol were also carried out by us. Previously, discussed that in two polar protic solvents (DMSO and THF) only the cationic form of NBA exists, it was also suggested by time-resolved measurements, as the decay profile of NBA best-fitted single exponentially for both water and methanol, at  $\lambda_{ex}=635$  nm. The lifetime of NBA in neat water is 0.35 ns which was exactly matched with the previous reports<sup>S4</sup> and after the addition of 17  $\mu\text{g/ml}$  GO it remains unchanged (Fig.S9a, Table.S1), indicated that the quenching of NBA fluorescence by GO is static in nature. Similarly in methanol, the lifetime of NBA is 1.18 ns after the addition of 85  $\mu\text{g/ml}$  GO it remains unchanged (Fig.S9b, Table.S1), indicated that the quenching of NBA fluorescence by GO is static in nature in water and methanol.

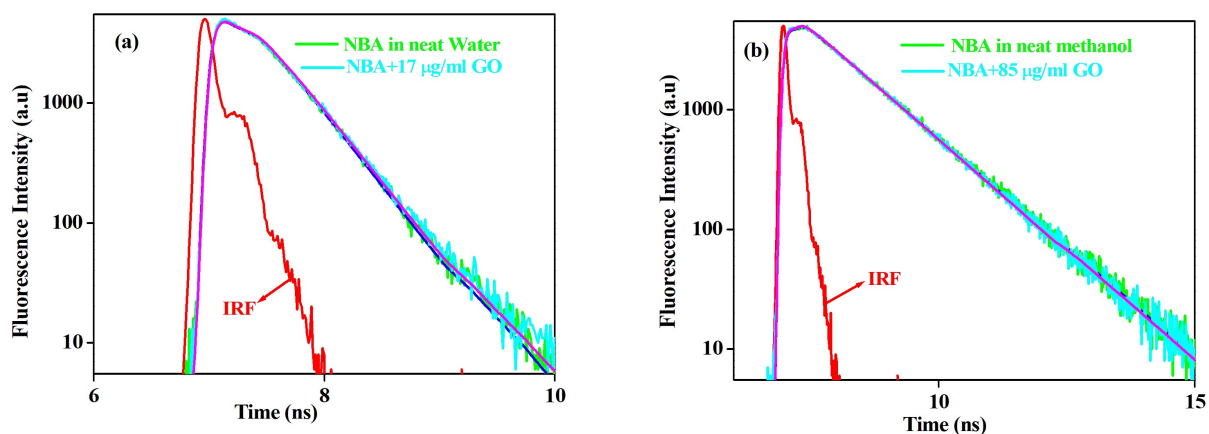


**Fig.S9** Time-resolved fluorescence emission decay traces of NBA in with gradual addition of GO at  $\lambda_{ex}=635$  nm (a) in water (b) in methanol.

**Table S1.** Time-resolved fluorescence emission decay parameters of NBA upon complexation with GO at  $\lambda_{ex}$ =635 nm in different solvent media.

System	$\lambda_{exi}$ (nm)	$\lambda_{emi}$ (nm)	$\tau_1/ns$ ( $a_1$ )	$\tau_2/ns$ ( $a_2$ )	$\tau_{av}$ (ns)	$\chi^2$
NBA in neat DMSO	635	680	0.22 (0.12)	1.39 (0.88)	1.25	1.12
NBA+ 15 $\mu$ g/ml GO in DMSO	635	680	0.20 (0.13)	1.38 (0.87)	1.23	1.20
NBA+ 90 $\mu$ g/ml GO in DMSO	635	680	0.22 (0.12)	1.37 (0.88)	1.23	1.16
NBA in neat THF	635	670	0.13 (0.19)	1.76 (0.81)	1.52	1.12
NBA+ 10 $\mu$ g/ml GO in THF	635	670	0.16 (0.15)	1.77 (0.85)	1.53	1.08
NBA+ 60 $\mu$ g/ml GO in THF	635	670	0.13 (0.17)	1.76 (0.83)	1.48	1.14
NBA in neat water	635	677	0.35 (1.00)	-	0.35	1.20
NBA+17 $\mu$ g/ml of GO in water	635	677	0.35 (1.00)	-	0.35	1.20
NBA in neat methanol	635	665	1.18 (1.00)	-	1.18	1.20
NBA+85 $\mu$ g/ml of GO in methanol	635	665	1.18 (1.00)	-	1.18	1.06

**Table S2.** Time-resolved fluorescence emission decay parameters of NBA upon complexation with GO at  $\lambda_{ex}$ =510 nm in different solvent media.

System	$\lambda_{exi}$ (nm)	$\lambda_{emi}$ (nm)	$\tau_1/ns$ ( $a_1$ )	$\tau_2/ns$ ( $a_2$ )	$\tau_2/ns$ ( $a_2$ )	$\tau_{av}$ (ns)	$\chi^2$
NBA in neat DMSO	510	610	0.05 (0.45)	1.44 (0.12)	2.30 (0.43)	0.88	1.09
NBA+ 15 $\mu$ g/ml GO in DMSO	510	610	0.05 (0.68)	1.86 (0.08)	4.10 (0.24)	1.16	1.13
NBA in neat THF	510	600	0.05 (0.62)	0.84 (0.32)	3.83 (0.06)	0.53	1.16
NBA+ 10 $\mu$ g/ml GO in THF	510	600	0.05 (0.59)	1.15 (0.05)	3.86 (0.36)	1.48	1.10

## 55. Raman spectral study in different solvent media.

Raman spectral study provides information about the interactions between GO with NBA in different solvent media. In the Raman spectra, GO shows two characteristic Raman bands around  $\sim 1600$  and  $\sim 1350$   $\text{cm}^{-1}$  region. The band around  $\sim 1600$   $\text{cm}^{-1}$  is known as G band. G band of GO is due to the in plane vibration mode of  $\text{sp}^2$  hybridized carbon atoms (first order scattering of the  $E_{2g}$  phonon).<sup>55</sup> Whereas, the band around  $\sim 1350$   $\text{cm}^{-1}$  region is known as D band of GO, which demonstrate the disordered  $\text{sp}^3$  hybridized carbon atoms.<sup>56</sup> In our study we have found that in neat DMSO the characteristics D and G bands of GO appears at 1350, 1596  $\text{cm}^{-1}$  region (**Fig.S10a**). When GO-NBA complex was formed in DMSO, the characteristics D and G bands of GO is shifted to the lower wavenumber region, and appears at 1344 and 1578  $\text{cm}^{-1}$  region (**Fig.S10b**). Similarly in neat THF the characteristics D and G bands of GO appears at 1346, 1586  $\text{cm}^{-1}$  region and that of GO-NBA complex appears at 1350, 1575  $\text{cm}^{-1}$  region (**Fig.S10b**). Here we found out that the D band shifted towards higher wavenumber region and G band shifted towards lower wavenumber region. In neat water, we found that the characteristics D and G bands of GO appears at 1347, 1592  $\text{cm}^{-1}$  region, and that of GO-NBA complex appears at 1352, 1578  $\text{cm}^{-1}$  region (**Fig.S10c**). However in the case of methanol we found similar kind of result like DMSO, here both D and G bands of GO-NBA complex shifted towards lower wavenumber region compared to that of GO in neat methanol (**Fig.S10d**).

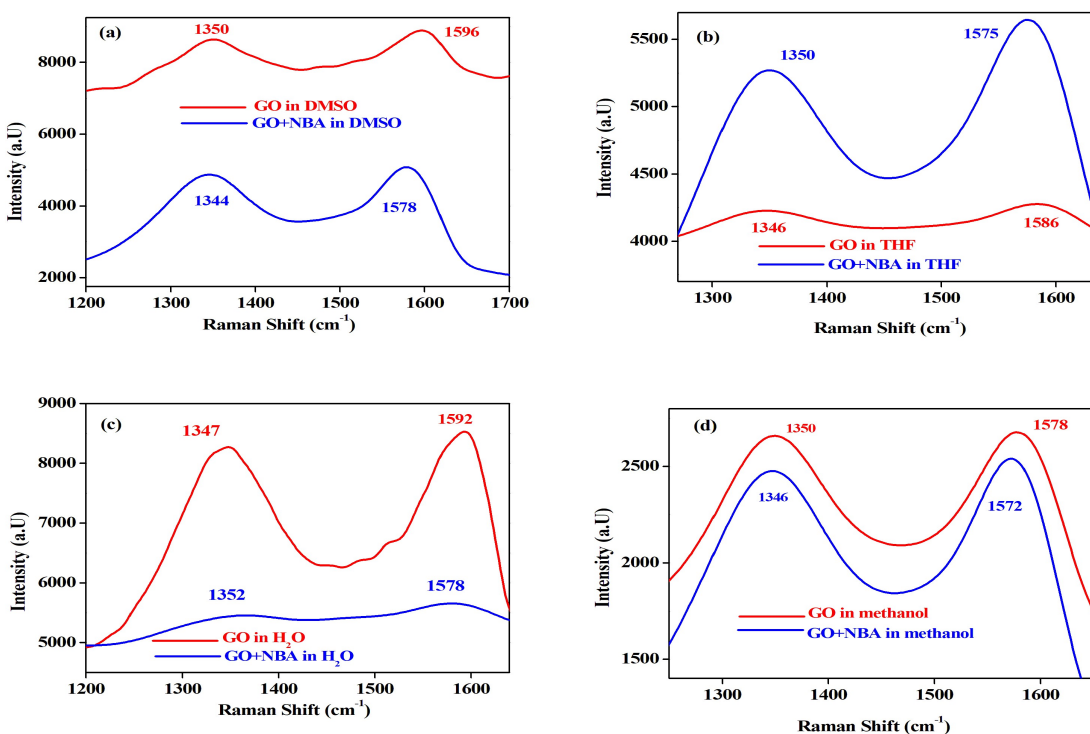
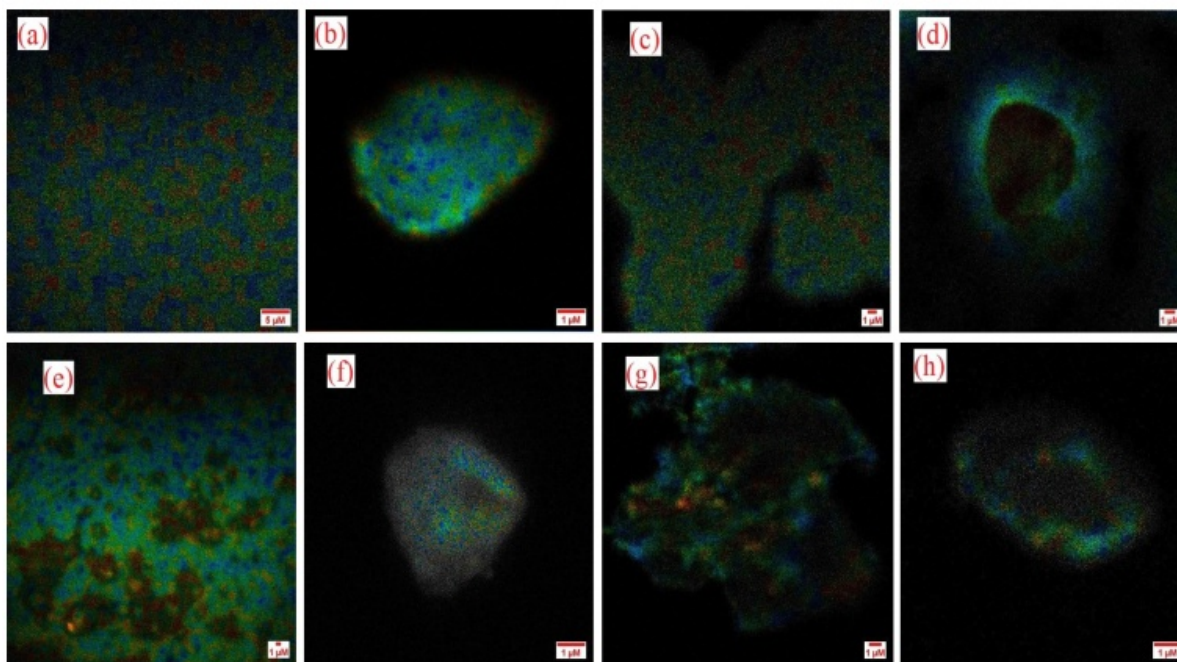


**Fig.S10** Raman spectra of GO and GO-NBA complex in (a) DMSO, (b) THF, (c) water and (d) methanol.

So it is noticeable that for all four solvent systems the characteristics G band of GO was shifted towards lower wavenumber region when it complexed with NBA. The D band of GO was shifted towards lower wavenumber region for DMSO and methanol and shifted towards higher wavenumber region for THF and water. This results indicates that the GO surface structure was modified due to the formation of additional chemical bonds between the carbon atoms of phenolic moieties of GO and the functional groups.<sup>56</sup>

#### 56. FLIM study of NBA-GO complex systems in different solvent media.

Fluorescence lifetime imaging (FLIM) study of NBA, in the presence of GO by varying the solvents, were carried out by us, to probe the interactions between GO and NBA in the different solvent media. It is a highly advanced spectroscopic technique, having several biomedical and biological applications.<sup>57,58</sup> It is well known that GO is not used for real-time FLIM imaging, as GO itself is weakly fluorescent. However when GO is interacted/conjugated with the fluorophores then only they may be visible during the imaging. Here we have studied the fluorescence lifetime imaging of NBA in different solvent media, also the NBA and GO conjugate in the different solvent media at  $\lambda_{ex}=635$  nm. In the absence of GO we found that for all four solvent media NBA was homogeneously distributed (Fig.S11 a,c,e,g). However, in the presence of GO, we found

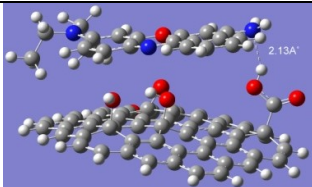
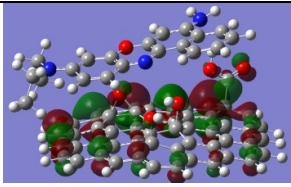
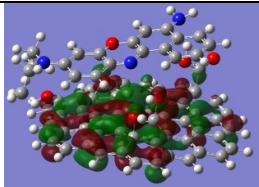
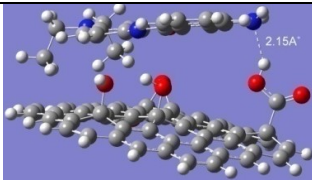
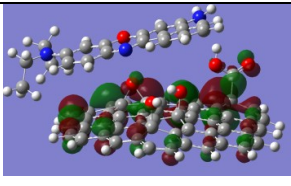
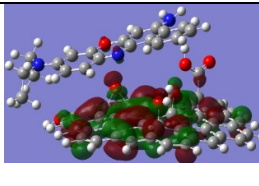
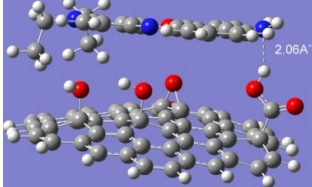
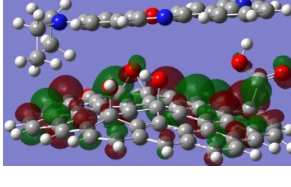
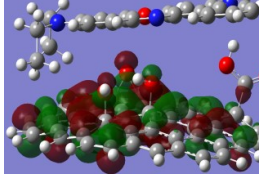
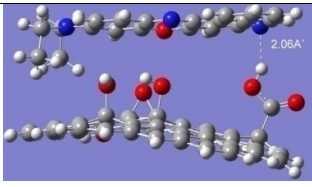
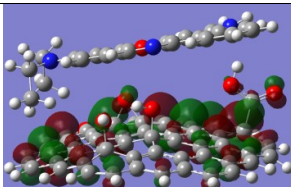
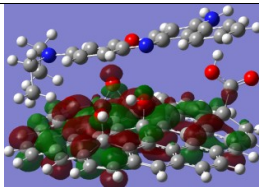
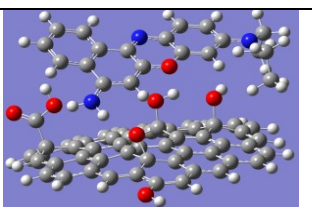
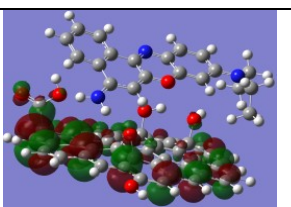
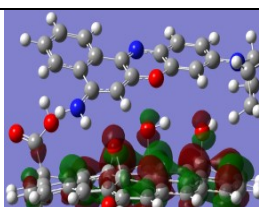


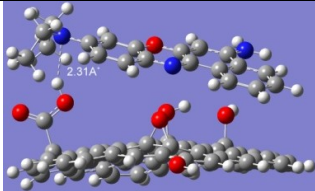
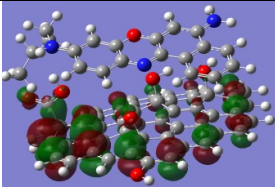
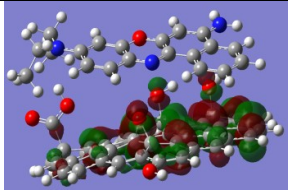
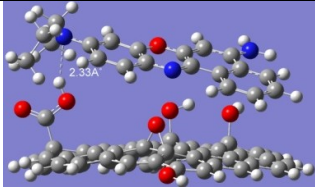
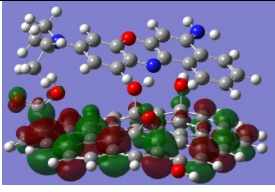
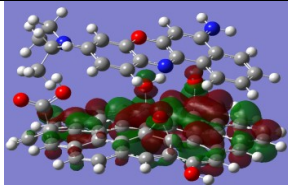
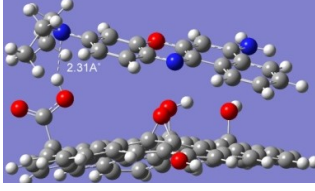
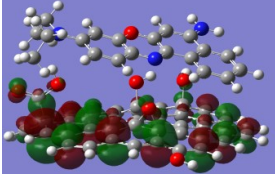
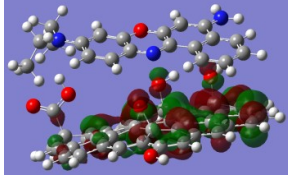
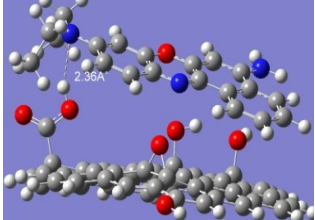
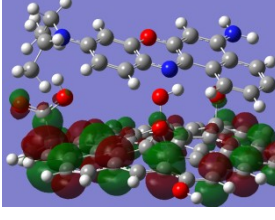
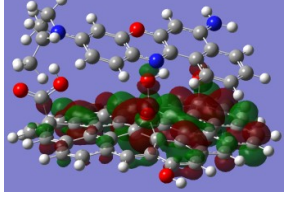
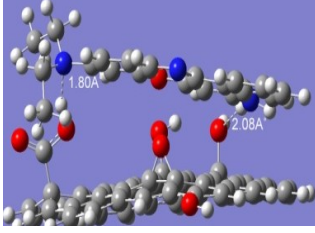
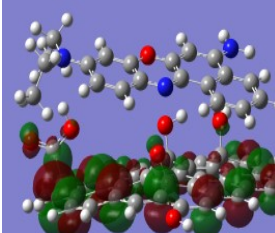
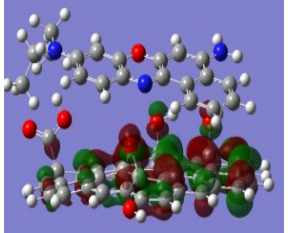
**Fig.S11** (a,c,e,g) are the FLIM images of NBA in DMSO, THF, H<sub>2</sub>O, and methanol respectively, (b,d,f,h) are the FLIM images of NBA-GO complex in DMSO, THF, H<sub>2</sub>O, and methanol respectively.

that NBA molecules were placed on the GO surface, and also the NBA fluorescence was quenched compare to NBA in neat solvent (Fig.S11 b,d,f,h). This study shows that the interaction of GO with NBA in all four studied solvent systems. When we

have excited our samples (NBA in neat DMSO, THF, and in presence of GO) by using 510 nm excitation source we have not found any images, corresponding to NBB.

**S7. Computational studies to probe the interaction of NBA, NBB with GO.**

Forward Orientation	HOMO	LUMO	Solvent
 <p>2.13Å<sup>1</sup></p>			Water
 <p>2.15Å<sup>1</sup></p>			Methanol
 <p>2.06Å<sup>1</sup></p>			DMSO
 <p>2.06Å<sup>1</sup></p>			THF
			Gas Phase

Reverse Orientation	HOMO	LUMO	Solvent
			Water
			Methanol
			DMSO
			THF
			Gas Phase

**Fig. S12** Optimized geometries of NBA: GO complexes (Forward and Reverse orientations) and their frontier molecular orbital pictures in different solvents studied and in gas phase.

**Table. S3 Internal energy, binding energy and the energy gap in between LUMO and HOMO of NBA: GO complexes in forward and reverse orientations, and NBB: GO complexes in different solvent media.**

System	Solvent	Energy (au)	BE (Kcal/Mol)	Dielectric Constant ( $\epsilon$ )	$\Delta E_{\text{Gap}}$ (eV)
NBA: GO complex in forward orientation	Water	-3573.54868	-98.806	80.1	2.110
	Methanol	-3573.54731	-99.462	46.7	2.123
	DMSO	-3573.54604	-97.885	20.7	2.040
	THF	-3573.53267	-98.365	7.6	1.859
NBA: GO complex in reverse orientation	Water	-3573.54928	-99.178	80.1	2.197
	Methanol	-3573.54663	-99.038	46.7	2.185
	DMSO	-3573.54796	-99.084	20.7	2.199
	THF	-3573.53492	-99.772	7.6	2.032
NBA: GO complex in forward orientation	Gas Phase	-3573.50458	-129.421	-	1.662
NBA: GO complex in reverse orientation	Gas Phase	-3573.50982	-132.707	-	1.637
NBB: GO complex	THF	-3572.94749	-19.718	7.6	3.400
	DMSO	-3572.95734	-19.861	20.7	3.388

#### References.

S1. M. J. Frisch, G. W. Trucks, H. B. Schlegel, G. E. Scuseria, M. A. Robb, J. R. Cheeseman, G. Scalmani, V. Barone, G. A. Petersson, H. Nakatsuji, X. Li, M. Caricato, A. V. Marenich, J. Bloino, B. G. Janesko, R. Gomperts, B. Mennucci, H. P. Hratchian, J. V. Ortiz, A. F. Izmaylov, J. L. Sonnenberg, D. Williams-Young, F. Ding, F. Lipparini, F. Egidi, J. Goings, B. Peng, A. Petrone, T. Henderson, D. Ranasinghe, V. G. Zakrzewski, J. Gao, N. Rega, G. Zheng, W. Liang, M. Hada, M. Ehara, K. Toyota, R. Fukuda, J. Hasegawa, M. Ishida, T. Nakajima, Y. Honda, O. Kitao, H. Nakai, T. Vreven, K. Throssell, J. A. Montgomery, Jr., J. E. Peralta, F. Ogliaro, M. J. Bearpark, J. J. Heyd, E. N. Brothers, K. N. Kudin, V. N. Staroverov, T. A. Keith, R. Kobayashi, J. Normand, K. Raghavachari, A. P. Rendell, J. C. Burant, S. S. Iyengar, J. Tomasi, M. Cossi, J. M. Millam, M. Klene, C. Adamo, R.

Cammi, J. W. Ochterski, R. L. Martin, K. Morokuma, O. Farkas, J. B. Foresman, and D. J. Fox, Gaussian, Inc., Wallingford CT, 2016.

S2. J. J. H. Rosas, R. E. R. Gutierrez, A. Escobedo-Morales and E. C. Anota, *J. Mol. Model.*, 2011, **17**, 1133-1139.

S3. H. Vovusha, S. Sanyal and B. Sanyal, *J. Phys. Chem. Lett.*, 2013, **4**, 3710-3718.

S4. G. B. Dutt, S. Doraiswamy, N. Periasamy and B. Venkataraman, *J. Chem. Phys.*, 1990, **93**, 8498-8513.

S5. F. Tuinstra and J. L. Koenig, *J. Chem. Phys.* 1970, **53**, 1126-1130.

S6. J. Yan, Y. Zhang, P. Kim and A. Pinczuk, *Phys. Rev. Lett.*, 2007, **98**, 166802.

S7. W. Becker., *J. Microsc.*, 2012, **247**, 119-136.

S8. J. R. Lakowicz, 3rd ed.; *Springer: New York*, 2006.